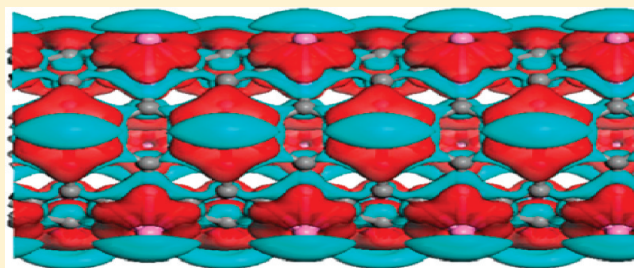


Enhanced Hydrogen Storage on Li Functionalized BC₃ NanotubeJian Zhou,[†] Qian Wang,[‡] Qiang Sun,^{*,†,‡} and Puru Jena[‡][†]Department of Advanced Materials and Nanotechnology, and Center for Applied Physics and Technology, Peking University, Beijing 100871, China[‡]Department of Physics, Virginia Commonwealth University, Richmond, Virginia 23284, United States

ABSTRACT: First principles calculations based on density functional theory are carried out to study the effect of lithium functionalization of experimentally synthesized BC₃ nanotube on charge transfer, electrostatic potential, and hydrogen storage. Electron-deficient BC₃ nanotube is found to promote charge transfer from Li to the substrate when lithiated. The resulting Li ions on the tube surface can effectively polarize hydrogen molecules and improve their binding energy and storage capacity. While each Li site on BC₃ nanotube is found to adsorb up to two H₂ molecules, zigzag nanotube shows better performance as a hydrogen storage material with good adsorption energy (0.11 eV/H₂) and high gravimetric density (6.9%). These data are consistent with the system target set by the DOE for 2010.



Currently, the biggest challenge in a new hydrogen economy is finding materials that can store hydrogen with high gravimetric and volumetric density under favorable thermodynamic conditions and possess fast kinetics. A considerable amount of experimental and theoretical research effort has been devoted to studying storage of hydrogen in various materials. Due to the high surface to volume ratio and the well-known tunable size-dependent properties of fullerene and carbon nanotubes (NTs), carbon based nanomaterials have received a great deal of attention.^{1–5} It has been demonstrated^{3–5} that pure carbon materials cannot be used for hydrogen storage because they interact weakly with hydrogen.

In order to improve the binding energy of hydrogen while maintaining the light weight of the storage material, doping of carbon with light metal atoms is desirable. Among these, Li doping seems to be promising since not only is it the lightest metal in the periodic table but also a positively charged Li⁺ ion in free space has been shown to store six hydrogen molecules with desirable adsorption energy.⁶ Li functionalized C₆₀ where 12 Li atoms are capped on the 12 pentagons was found to store hydrogen with large gravimetric density.⁷ Here, six electrons from the Li atoms are transferred to the threefold degenerate LUMO of C₆₀, and each Li atom carries a charge of 0.5 electrons. This partial charge transfer resulted in a hydrogen adsorption energy of 0.075 eV/H₂.⁷ This binding is weak for Li₁₂C₆₀ to serve as a hydrogen storage material for room temperature and ambient pressure⁸ applications. To further improve this adsorption energy, it was shown that substitutional doping of B at the C site in C₆₀ may be effective.⁹ When some of the C atoms are replaced by B atoms, the system becomes electron-deficient. Consequently, more electrons can be transferred from the Li atoms to the C₆₀ substrate leaving Li ions in a more positively charged state. Thus, the enhanced local electric field produced

by these ions can significantly improve the adsorption. Indeed, the hydrogen adsorption energy in Li₁₂C₄₈B₁₂ can reach 0.135 eV/H₂,⁹ which lies in the desirable energy window.¹⁰ However, C₄₈B₁₂ has not yet been synthesized, and up to six C atoms in C₆₀ have been replaced by B. From a practical point of view, it will be ideal to have a substrate which already has been synthesized and can be doped by Li. In this regard BC₃ nanotube (NT) is a good candidate which has been synthesized experimentally¹¹ through chemical reactions. Further, it has been found that Li absorption can be enhanced with B doping on carbon NT.¹²

In this paper we report first principles calculations, based on density functional theory, of hydrogen adsorption in Li decorated BC₃ NT. We focus on the following questions: (1) Where do Li atoms bind and distribute on BC₃ NT and how does this depend upon different chiralities of the substrate? (2) How strong is the binding of Li and how does it change with tube radius? (3) How different are the hydrogen gravimetric densities for armchair (A-) and zigzag (Z-) BC₃ NT? We show that the distribution and binding of Li as well as the hydrogen gravimetric density depend on the chirality of BC₃ NT and that Z-BC₃ NT is better than A-BC₃ NT for hydrogen storage.

Calculations were carried out using density functional theory (DFT) and the generalized gradient approximation (GGA)¹³ for the exchange and correlation functional. We used the Perdew–Wang (PW91)¹⁴ form for the GGA. All computations were carried out using the Vienna Ab Initio Simulation Package (VASP),¹⁵ the ultrasoft pseudopotentials, and a plane-wave basis set with the projector augmented plane-wave method (PAW).¹⁶ Periodic boundary condition and vacuum space of ~15 Å along

Received: November 19, 2010

Revised: February 12, 2011

Published: March 09, 2011

x - and y -directions were applied in order to avoid interactions between two images of BC_3 NTs. The structures were relaxed using the gradient conjugated method with no symmetric constraints. To represent reciprocal space, Monkhorst–Pack k points¹⁷ of $1 \times 1 \times 7$ mesh are used. Denser k point meshes will affect the total energy within 0.002 eV. The energy cutoff, convergence criteria of energy, and force are set to be 400 eV, 1×10^{-4} eV, and 0.02 eV/Å, respectively. The accuracy of our calculation was tested by computing the H_2 bond length and dissociation energy, which are, respectively, 0.749 Å and 4.50 eV and agree well with the experimental value, namely, 0.741 Å and 4.53 eV. We also calculated geometric and electronic structures of the BC_3 sheet. Calculated B–C and C–C bond lengths of 1.564 and 1.421 Å, respectively, agree with previous results.¹⁸

First, we study the site preference of Li on BC_3 NT with varying chiralities. Calculations are carried out for the armchair type (n, n) ($n = 4, 6, 8$) and the zigzag type $(m, 0)$ ($m = 6, 8, 10$) NTs. The indices m and n are even since BC_3 sheet has a 2×2 reconstruction. Structural optimizations show that nanotubes

can still retain their circular cross section after B doping, and the relaxed B–C and C–C bond lengths are ~ 1.56 and ~ 1.42 Å, respectively, similar to those of BC_3 sheet. It has been reported that Li atom prefers to reside on the hollow site over C hexagonal ring^{19–21} in pure C nanotube, and its binding can be further enhanced when B atoms are doped in the hexagonal ring.^{12,22} Note that there are three different kinds of hollow sites on BC_3 NT where Li atoms can reside, namely, H_A , H_B , and H_C , as shown in Figure 1. There are two B atoms in each of the hexagonal H_A and H_B sites, while the H_C hexagonal site is composed of C atoms only. Therefore, we just consider the adsorption sites marked H_A and H_B sites in our calculations. When one Li atom is introduced to the H_A or H_B site and the geometries are allowed to relax, we find that the H_A site is more favorable than the H_B site by 0.12 eV for the (4, 4) NT and 0.4 eV for the (6, 0) NT. The corresponding structures for Li doped BC_3 NT are shown in Figure 1c and d. Different energies are due to different chiralities and curvatures of the NTs. The absorption energy of Li atom on the H_A site is found to be 2.53 eV for (4, 4) and 2.42 eV for (6, 0) BC_3 NT.

Now we introduce a second Li atom to neighboring sites of H_A in order to investigate how successive Li atoms will be distributed on the BC_3 NT. We found that the second Li atom still prefers a H_A -type site for both A- BC_3 NT and Z- BC_3 NT over the H_B -type site by 0.20 and 0.45 eV, respectively (Figure 1e and f). Based on these findings, we introduce Li atoms to all H_A -type sites of A- BC_3 NT and Z- BC_3 NT (Figure 1g and h).²³ The average Li–B and Li–C bond lengths on (4, 4) BC_3 NT are calculated to be 2.31 and 2.14 Å, respectively, while for (6, 0) BC_3 NT, the corresponding values are 2.27 and 2.12 Å. In Table 1 we list the calculated distances between Li–Li and Li–B, average adsorption energy per Li atom, charge on the Li atom, and average binding energy per H_2 . From these data the following conclusions can be drawn: (1) Concentration of Li on BC_3 NT depends on the tube's chirality. The atomic ratios of Li to B and C are 1/8 and 1/4 for A- and Z- BC_3 NT, respectively. This is larger than previous studies of Li dispersed on pure CNT.²¹ (2) Li atoms on Z- BC_3 NT are distributed more densely than those on A- BC_3 NT. For example, in the x - and y -direction Li–Li distances R_1 are 3.95 and 3.59 Å for (6, 0) and (10, 0) BC_3 NTs, respectively. The distance in the z -direction, R_2 , on the other hand, is 4.42 Å for all three Z- BC_3 NTs. In A- BC_3 NT, R_1 ranges from 6.11 to 6.61 Å, while R_2 is 5.12 Å. Both these distances are larger than those in Z- BC_3 NT. (3) The distance between Li and B as well as the charge transfer from Li decrease slightly with increasing diameter. (4) The average adsorption energy of Li increases with tube diameters of Z- BC_3 NT. This is due to the reduction in the Li–B distance.

In the following we discuss the charge transfer from the Li atom to BC_3 NT as the positive Li ion is expected to polarize and bind the H_2 molecule. Charge analysis by integrating electrons

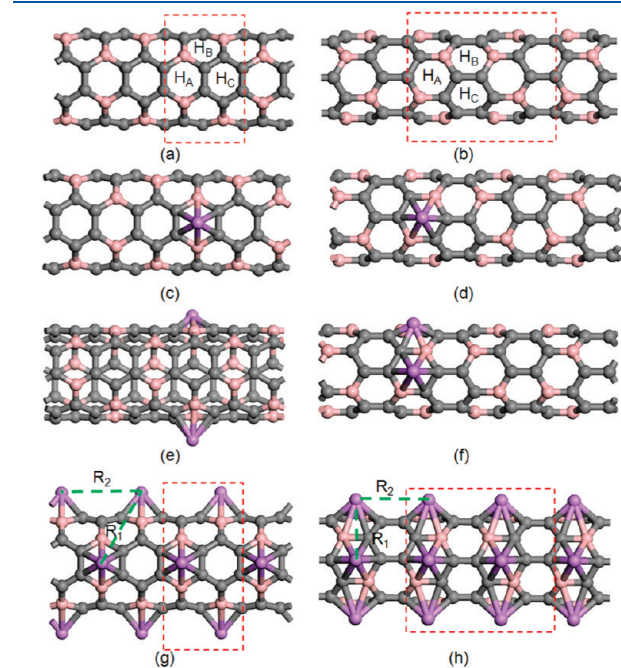


Figure 1. Structures of (a) (4, 4) BC_3 NT and (b) (6, 0) BC_3 NT, (c) 1 Li on (4, 4) BC_3 NT and (d) 1 Li on (6, 0) BC_3 NT, (e) 2 Li atoms on (4, 4) BC_3 NT and (f) 2 Li atoms on (6, 0) BC_3 NT, (g) 4 Li atoms on (4, 4) and (h) 12 Li atoms on (6, 0) BC_3 NT. R_1 and R_2 are distances between Li atoms. Simulated unit cells are represented by dashed rectangles in (a), (b), (g), and (h). For (c) and (e) the simulated supercell is a triple unit cell; for (d) and (f) the supercell is a double unit cell.

Table 1. Atomic Ratio of Li to B and C, Average Distance Li–Li (R_1) and Li–B (R) (in Å), Average Adsorption Energy per Li on BC_3 NT (E_b/Li , in eV), Charge on Li (Q_Li , in electrons), and Average Binding Energy per H_2 on Li (E_b/H_2 , in eV)

| | 4Li-(4, 4) BC_3 NT | 6Li-(6, 6) BC_3 NT | 8Li-(8, 8) BC_3 NT | 12Li-(6, 0) BC_3 NT | 16Li-(8, 0) BC_3 NT | 20Li-(10, 0) BC_3 NT |
|-------------------------|-----------------------------|-----------------------------|-----------------------------|------------------------------|------------------------------|-------------------------------|
| ratio | 1/8 | 1/8 | 1/8 | 1/4 | 1/4 | 1/4 |
| R_1 | 6.61 | 6.33 | 6.11 | 3.95 | 3.69 | 3.59 |
| R | 2.34 | 2.30 | 2.28 | 2.30 | 2.27 | 2.25 |
| E_b/Li | 2.42 | 2.42 | 2.42 | 2.24 | 2.28 | 2.30 |
| Q_Li | +0.63 | +0.62 | +0.61 | +0.60 | +0.59 | +0.58 |
| E_b/H_2 | 0.10 | 0.09 | 0.09 | 0.11 | 0.11 | 0.11 |

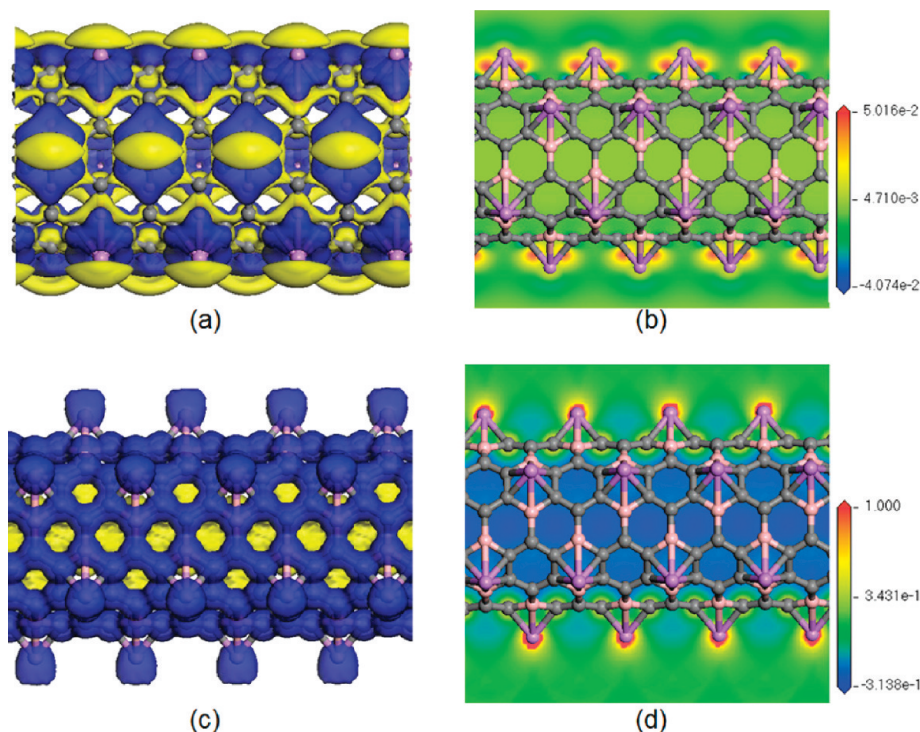


Figure 2. (a) Isosurface with value of 0.012 electron/Å³ and (b) 2D contour of transferred electron density ($\rho_{\text{Li-BC}_3\text{NT}} - \rho_{\text{Li}} - \rho_{\text{BC}_3\text{NT}}$), (c) isosurface with value of 0.2 electron/Å³ and (d) 2D contour of electrostatic potential of 6Li-(6, 6) BC₃ NT. Blue and yellow colors correspond to positive and negative values.

inside the Wigner–Seitz cell of each Li atom showed that charges are transferred from Li to the tube substrate, and transferred charge is mainly located on the hexagon just below Li. Charge on A-BC₃ NT is slightly larger than those of Z-BC₃ NT. To visualize it more clearly, we calculated the transferred electron density ($\rho_{\text{Li-BC}_3\text{NT}} - \rho_{\text{Li}} - \rho_{\text{BC}_3\text{NT}}$) in Li doped on (6, 6) BC₃ NT. The resulting isosurface is plotted in Figure 2a and b in the form of a 2D contour. The blue and yellow curves indicate positive and negative charge density corresponding to electron accumulation and depletion, respectively. To further understand the effect of B doping of the carbon NT, some comparisons should be made between Li decorated on BC₃ NT and pure CNT. Recall that the average adsorption energy per Li on pure CNT was calculated to be 1.8 eV using LDA²⁰ and 1.5 eV using GGA.²¹ Our results (2.2–2.4 eV) indicate that B doping in CNT enhances the adsorption of Li and hence makes Li more positively charged (+0.6 e) than on pure CNT (+0.35 e using LDA²⁰ and +0.45 e using GGA²¹). Enhanced charge transfer due to B doping can lead to a stronger local electric field produced by the Li anion and hence can lead to stronger binding of the H₂ molecule. Since the electric field is the gradient of electrostatic potential and vertical to the isosurface, it is helpful to analyze the electrostatic potential. This is plotted in Figure 2 c and d for Li-(6, 6) BC₃ NT. We see that electrostatic potential is positive with large gradient near the outer tube while it is negative with small gradient in the inner tube. Therefore, the electric field in the outer tube would be larger than that of the inner tube, and H₂ molecules would preferably bind to the outer surface.

We also calculated the partial density of states (PDOS) in fully decorated Li on (4, 4) and (6, 0) BC₃ NTs (Figure 3). The systems are metallic-like with p electrons across the Fermi level. This is consistent with previous results.²⁴ It is known that pure

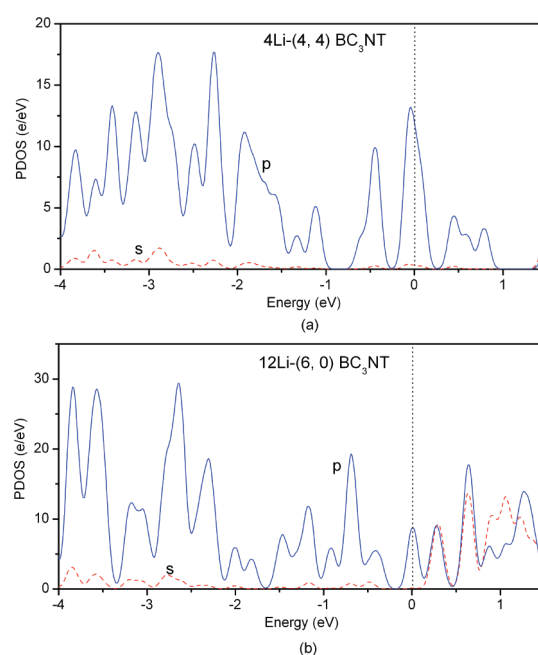


Figure 3. Calculated PDOS of (a) 4Li-(4, 4) BC₃ NT and (b) 12Li-(6, 0) BC₃ NT.

(4, 4) and (6, 0) carbon NTs are metallic-like. They become semiconducting when doped with B but become metallic again when Li atoms are introduced.

Finally we discuss hydrogen adsorption on Li functionalized BC₃ NT. Although previous studies^{12,19–22} show that each Li can

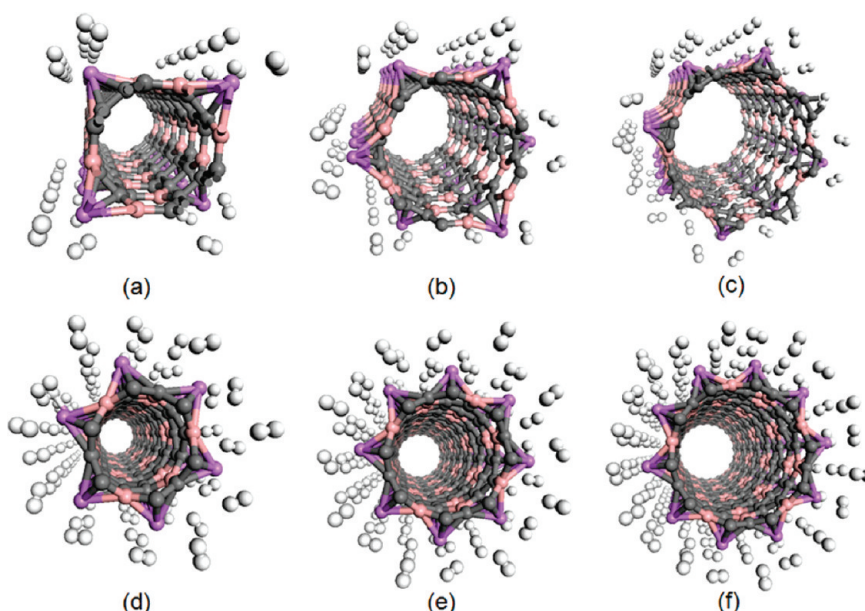


Figure 4. Relaxed structure of (a) 4Li-(4, 4) BC₃ NT-8H₂, (b) 6Li-(6, 6) BC₃ NT-12H₂, (c) 8Li-(8, 8) BC₃ NT-16H₂, (d) 12Li-(6, 0) BC₃ NT-24H₂, (e) 16Li-(8, 0) BC₃ NT-32H₂, and (f) 20Li-(10, 0) BC₃ NT-40H₂.

adsorb up to three or four H₂ molecules, we find that in the present system, due to steric hindrance, it is impossible to store more than two H₂ molecules on each Li site. The average binding energies per H₂ are shown in Table 1. These lie in the range of 0.09–0.11 eV/H₂. The binding energy of H₂ on Z-BC₃ NT is slightly larger than that in A-BC₃ NT although charges of Li site on Z-BC₃ NT are slightly smaller. This can be understood from the different distribution of Li on BC₃ NT. Compared to A-BC₃ NT, the Li–Li distance in Z-BC₃ NT is shorter, and accordingly the total electric field in the outer tube space would be stronger due to superposition. The geometric structures of H₂ adsorbed on Li functionalized A-BC₃ NT and Z-BC₃ NT are plotted in Figure 4. The relaxed average H₂ bond length is ~ 0.76 Å, which is only marginally larger than that in its free state, namely, 0.749 Å. This elongation results from electrostatic polarization of H₂. The distance between Li and H₂ is around 2.0–2.2 Å, which is consistent with the previously reported Li–H₂ distance.^{12,19–22} Since van der Waals interactions are not included, the GGA exchange correlation usually underestimates the binding energy²⁵ by ~ 0.08 eV/H₂. Thus, our predicted binding energy (0.09–0.11 eV/H₂) can actually be around 0.17–0.19 eV/H₂. Bhatia and Myers studied the optimum thermodynamic conditions for hydrogen adsorption employing the Langmuir equation and then derived relationships between the operating pressure of a storage tank and the enthalpy of adsorption required for storage near room temperature.²⁶ They have found that the average optimal adsorption enthalpy should be 15.1 kJ/mol, if operated between 1.5 and 30 bar at 298 K. When the pressure is increased to 100 bar, the optimal value becomes 13.6 kJ/mol. Therefore, for the systems studied here, the adsorption energy of H₂ falls in the required window of hydrogen storage under ambient environment. Furthermore, the gravimetric densities of hydrogen are 3.8 and 6.9 wt %, for A-BC₃ NT and Z-BC₃ NT, respectively, and result from different concentrations of Li on BC₃ NT as pointed out above. The latter satisfies the target set by the DOE for 2010.

In summary, we have studied the hydrogen storage properties of Li functionalized BC₃ NTs using density functional theory. From a detailed analysis of charge density distribution, electrostatic potential, and hydrogen adsorption, we have arrived at the following conclusions: (1) Li atoms bind to the hexagonal rings containing B atoms. (2) The binding energy of Li to B doped carbon nanotubes is larger than that in pure carbon nanotube. (3) The charge transfer from Li to the nanotube surface is enhanced once the carbon nanotube is doped with B. (4) The electric field strength along the outer tube surface of BC₃ NT is larger than that along the inner surface and hence becomes the preferred space for hydrogen molecules to bind. (5) Li functionalized zigzag BC₃ NT shows better hydrogen adsorption energy and higher gravimetric density than Li functionalized armchair BC₃ NT. (6) Lithiation not only improves the performance of hydrogen storage of BC₃ NT but also changes its electronic structure resulting in metallic behavior. Since BC₃ NTs have been experimentally synthesized, our theoretical prediction is expected to stimulate experimental studies of hydrogen adsorption by functionalizing the nanotube with lithium.

AUTHOR INFORMATION

Corresponding Author

*E-mail sunqiang@pku.edu.cn.

ACKNOWLEDGMENT

This work is partially supported by grants from the National Natural Science Foundation of China (10874007, 20973010), the National Grand Fundamental Research 973 Program of China (2010CB631301), and by the U.S. Department of Energy.

REFERENCES

- (1) Dillon, A. C.; Jones, K. M.; Bekkedahl, T. A.; Kiang, C. H.; Bethune, D. S.; Heben, M. J. *Nature* **1997**, *368*, 377.

- (2) Tibbetts, G. G.; Meisner, C. P.; Olk, C. H. *Carbon* **2001**, 39, 2291.
- (3) Shiraishi, M.; Takenobu, T.; Ata, M. *Chem. Phys. Lett.* **2003**, 367, 633.
- (4) Kajiura, H.; Tsutsui, S.; Kadono, K.; Kakuta, M.; Ata, M.; Murakami, Y. *Appl. Phys. Lett.* **2003**, 82, 1105.
- (5) Dodziuk, H.; Dolgonos, G. *Chem. Phys. Lett.* **2002**, 356, 79.
- (6) Rao, B. K.; Jena, P. *Europhys. Lett.* **1992**, 20, 307. Niu, J.; Rao, B. K.; Jena, P. *Phys. Rev. Lett.* **1992**, 68, 2277.
- (7) Sun, Q.; Jena, P.; Wang, Q.; Marquez, M. *J. Am. Chem. Soc.* **2006**, 128, 9741.
- (8) <http://www1.eere.energy.gov/hydrogenandfuelcells/storage/index.html>.
- (9) Sun, Q.; Wang, Q.; Jena, P. *Appl. Phys. Lett.* **2009**, 94, 013111.
- (10) Bhatia, S.; Myers, A. L. *Langmuir* **2006**, 22, 1688.
- (11) Fuentes, G. G.; Borowiak-Palen, E.; Knupfer, M.; Pichler, T.; Fink, J.; Wirtz, L.; Rubio, A. *Phys. Rev. B* **2004**, 69, 245403.
- (12) Wu, X.; Gao, Y.; Zeng, X. C. *J. Phys. Chem. C* **2008**, 112, 8458.
- (13) Perdew, J. P.; Burke, K.; Ernzerhof, M. *Phys. Rev. Lett.* **1996**, 77, 3865.
- (14) Wang, Y.; Perdew, J. P. *Phys. Rev. B* **1991**, 44, 13298.
- (15) Kresse, G.; Furthmüller, J. *Phys. Rev. B* **1996**, 54, 11169.
- (16) Kresse, G.; Joubert, D. *Phys. Rev. B* **1999**, 59, 1758.
- (17) Monkhorst, H. J.; Pack, J. D. *Phys. Rev. B* **1976**, 13, 5188.
- (18) Wang, Q.; Chen, L.; Annett, J. F. *Phys. Rev. B* **1996**, 54, 2271.
- (19) Froudakis, G. E. *Nano Lett.* **2001**, 1, 531.
- (20) Liu, W.; Zhao, Y. H.; Li, Y.; Jiang, Q.; Lavernia, E. J. *J. Phys. Chem. C* **2009**, 113, 2028.
- (21) Ni, M.; Huang, L.; Guo, L.; Zeng, Z. *Int. J. Hydrogen Energy* **2010**, 35, 3546.
- (22) Liu, C.; Zeng, Z. *Appl. Phys. Lett.* **2010**, 96, 123101.
- (23) Actually, we have also calculated the structure that Li decorated on all H_A and H_B sites; however, each Li cannot adsorb even one H₂ due to too high concentration of Li decoration.
- (24) Zhou, Z.; Zhao, J.; Gao, X.; Chen, Z.; Yan, J.; Schleyer, P.; von, R.; Morinaga, M. *Chem. Mater.* **2005**, 17, 992.
- (25) Grimme, S. *J. Comput. Chem.* **2004**, 25, 1463.
- (26) Bhatia, S. K.; Myers, A. L. *Langmuir* **2006**, 22, 1688.